ÓPTICA PURA Y APLICADA
www.sedoptica.es

Type: RESEARCH PAPER
Section: BIOPHOTONICS/MEDICAL OPTICS

Applications in light-induced spectroscopy with violet LED lamp: autofluorescence

Aplicaciones de espectroscopía inducida por luz LED violeta: autofluorescencia

M.E. Etcheverry[1,3*], M.A Pasquale[2,3], M. Garavaglia[1,3]

1. Centro de Investigaciones Ópticas (CCT-CONICET La Plata, UNLP and CIC-BA), Gonnet, La Plata, Argentina.

2. Instituto de Investigaciones Fisicoquímicas Teóricas y Aplicadas (INIFTA), CONICET, Facultad de Ciencias Exactas, Departamento de Química, UNLP, La Plata, Argentina

3. Facultad de Ciencias Exactas, Universidad Nacional de La Plata, Argentina

(*) E-mail: mariaeugeniae@ciop.unlp.edu.ar

Received: 30/11/2022 Accepted: 22/09/2023
DOI: 10.7149/OPA.56.3.51120

ABSTRACT:

The early detection of a neoplastic disease, as well as the development of more efficient treatments, are crucial for improving the survival rate. A variety of new and emerging diagnostic strategies based on spectroscopic techniques such as non-invasive one-point fluorescence (PF) detection, are available to improve the screening procedure [1,2]. PF technique provides useful information for monitoring the evolution of the abundance and distribution of endogenous fluorophores associated with the neoplastic disease in low-pigmented superficial neoplasia [3,4].

The main objective of the present study was to develop a violet LED light source suitable for medical application devoted to the diagnostic and treatment of non-melanoma skin cancers. For this propose, we constructed a 12 W violet LED lamp (with maximum emission peak at 405 nm) made up of four mobile 3 W LED, each one coupled to a heat sink and a lens and mounted on a platform with adjustable screws. The power supply allows the modification of the intensity of illumination. The LED lamp was characterized employing a spectrometer coupled to an optical fiber. The irradiance for different distances between the lamp and the detector was assessed. Furthermore, the radiant power and the radiant intensity were evaluated. Data were compared with a simulated LED lamp by using the Zemax optic software for the realization of luminaries with the desired characteristics and modes of operation to deliver the energy density at the interest point, as required for medical applications.
The developed lamp in combination with a portable spectrometer was employed under medical supervision to detect differences in the emission spectrum of skin suspicious regions and healthy ones located at the head of a patient with non-melanoma skin cancer. The light of the LED lamp was concentrated in the examined region by means of the proper focusing of the four individual LEDs, rendering a high intensity homogeneous spot. Thus, endogenous chromophores at the skin were excited, and the emission intensity appeared to be enough to detect an enhanced peaked structure around 600 nm for some suspicious regions before treatment, and that were absence in healthy regions. These differences can be related to the augmented protoporphyrin IX content in neoplastic regions. Results presented in this work indicate the usefulness of the developed and characterized LED lamp as an easy-to-use device for the non-invasive detection of skin neoplastic pathologies, before and after treatment, with the aim of better define the malignant regions as well as predict the outcome of a certain treatment.

Key words: Non-melanoma skin cancer, one-point fluorescence detection, violet LED lamp.

RESUMEN:

La detección precoz de enfermedades neoplásica, así como el desarrollo de tratamientos más eficaces,

son cruciales para mejorar la tasa de supervivencia. Una variedad de nuevas y emergentes estrategias diagnósticas, basadas en técnicas espectroscópicas mínimamente invasivas, como la detección de fluorescencia puntual (PF), están disponibles para mejorar el procedimiento de detección [1,2]. La técnica de PF proporciona información útil para monitorear la evolución de la abundancia y distribución de fluoróforos endógenos asociados con la enfermedad neoplásica en neoplasias superficiales de baja pigmentación [3,4].

El objetivo principal del presente estudio fue desarrollar una fuente de luz LED violeta adecuada para aplicaciones médicas dedicadas al diagnóstico y tratamiento de cánceres de piel no melanoma. Para esto, construimos una lámpara LED violeta de 12 W (con pico máximo de emisión a 405 nm) compuesta por cuatro LED móviles de 3 W cada uno, acoplados a un disipador y una lente, y montada sobre una plataforma con tornillos ajustables. La fuente de alimentación permite modificar la intensidad de iluminación. La lámpara LED se caracterizó empleando un espectrofotómetro acoplado a una fibra óptica. Se evaluó la irradiancia para diferentes distancias entre la lámpara y el detector. Además, se evaluaron la potencia radiante y la intensidad radiante. Los datos se compararon con una lámpara LED simulada utilizando el software óptico Zemax para la realización de luminarias con las características y modos de operación deseados para entregar la densidad de energía en el punto de interés, según lo requerido para aplicaciones médicas. La lámpara desarrollada, en combinación con un espectrofotómetro portátil, se empleó, bajo supervisión médica, para detectar diferencias entre los espectros de emisión de regiones cutáneas sospechosas y sanas ubicadas en la cabeza de un paciente con cáncer de piel no melanoma. La luz de la lámpara LED se concentró en la región examinada mediante el enfoque adecuado de los cuatro LED individuales, lo que generó un área homogénea de alta intensidad. Por lo tanto, se excitaron cromóforos endógenos en la piel y la intensidad de la emisión resultó suficiente para detectar una estructura de picos alrededor de 600 nm para algunas regiones sospechosas antes del tratamiento. Esta estructura de picos está ausente en las regiones sanas, y puede estar relacionada con el aumento en el contenido de protoporfirina IX en las regiones neoplásicas.

Los resultados presentados en este trabajo indican la utilidad de la lámpara LED aquí desarrollada y caracterizada, como un dispositivo fácil de usar para la detección no invasiva de patologías neoplásicas de la piel, y con el objetivo de definir mejor las regiones malignas y predecir el resultado de un determinado tratamiento.

Palabras clave: Cáncer de piel no melanoma, detección de fluorescencia puntual, lámpara LED violeta

REFERENCES AND LINKS / REFERENCIAS Y ENLACES

[1] Q. Liu, "Role of Optical Spectroscopy Using Endogenous Contrasts in Clinical Cancer Diagnosis," World J Clin Oncol **10**, 50-63 (2011).

[2] D. van Straten, V. Mashayekhi, H.S. de Bruijn, S. Oliveira, D.J. Robinson, "Oncologic Photodynamic Therapy: Basic Principles, Current Clinical Status and Future Directions," Cancers (Basel) **9**(19)**,** 2-54 (2017).

[3] E. Borisova, L. Avramov, P. Pavlova, E. Pavlova, P. Troyanova, "Qualitative Optical Evaluation of Malignancies Related to Cutaneous Phototype," Proc. SPIE –Dynamics and Fluctuations in Biomedical Photonics VII, 75630X (2010).

[4] M. Panjepour, C. Julius, M. Phan, T. Vo-Dinh, S. Overholt, "Laser-induced Fluorescence Spectroscopy for in vivo Diagnosis of Non-melanoma Skin Cancers," Lasers Surg Med **31**, 367-373 (2002).

[5] J. Bigio, J.R. Mourant, "Ultraviolet and Visible Spectroscopies for Tissue Diagnostics: Fluorescence Spectroscopy and Elastic-scattering Spectroscopy," Phys Med Biol **42**, 803-814 (1997).

[6] R. Na, I. Stender, H. Wulf, "Can Autofluorescence Demarcate Basal Cell Carcinoma from Normal Skin? A Comparison with Protoporphyrin IX Fluorescence," Acta Derm-Venerol **81**, 246-249 (2001).

[7] A. Pena, M. Strupler, T. Boulesteix, G. Godeau, M.-C. Schanne-Klein, "Spectroscopic Analysis of Keratin Endogenous Signal for Skin Multiphoton Microscopy," Opt Express **13**, 6268-6274 (2005).

[8] N. Ramanujam, "Fluorescence Spectroscopy of Neoplastic and Non-neoplastic Tissues," Neoplasia **2**, 89-117 (2000).

[9] A. Leunig, K. Rick, H. Stepp, R. Gutmann, G. Alwin, R. Baumgartner, J. Feyh, "Fluorescence imaging and spectroscopy of 5-aminolevulinic acid induced Protoporphyrin IX for the dectection of neoplastic lesions in the oral cavity," Am J Surg **172**, 674-677 (1996).

[10] H. Kostron, A. Zimmermann, A. Obwegeser, "mTHPC-mediated photodynamic detection for fluorescence-guided resection of brain tumors," Proc SPIE **3262**, Surgical-Assist Systems (1998).

[11] J.S. Tyrrell, S.M. Campbell, A.Curnow A, "The relationship between protoporphyrin IX photobleaching during real-time dermatological methyl-aminolevulinate photodynamic therapy (MAL-PDT) and subsequent clinical outcome," Lasers Surg Med **42**,613-619 (2010).

[12] G.A. Wagnières, W.M. Star, B.C. Wilson, "In vivo fluorescence spectroscopy and imaging for oncological applications," Photochem Photobiol **68**, 603-632(1998).

[13] E. Borisova, L. Avramov, "Laser System for Optical Biopsy and in vivo Study of the Human Skin," Proc SPIE **4397**, 405-409 (2000).

[14] L. Bachmann, D. Zezell, A. da Costa Ribeiro, L. Gomes, A. Ito, "Fluorescence Spectroscopy of Biological Tissues," Appl Spectr Rev **41**, 575-590 (2006).

[15] R.E. Fischer, B. Tadic-Galeb, P.R. Yoder, Optical System Design, 2nd ed., McGraw-Hill, New York, (2008).

[16] W.J. Smith, Modern Optical Engineering, 4th ed., McGraw-Hill, United State, (2007).

[17] J.M. Geary, Introduction to Lens Design: With Practical Zemax Examples. Willmann-Bel, (2002).

[18] I. Moreno, C-C. Sun, "Modeling the radiation pattern of LEDs," Opt Express **16**,1808-1819 (2008).

[19] K.R. Rollakanti, S.C. Kanick, S.C. Davis, B.W. Pogue, E.V. Maytin, "Techniques for fluorescence detection of protoporphyrin IX in skin cancers associated with photodynamic therapy," Photonics Lasers Med **2**, 287-303 (2013)

[20] N. Rajaram, D. Kovacic; M.F. Migden, J.S. Reichenberg, T.H. Nguyen, J.W. Tunnell, "In vivo determination of optical properties and fluorophore characteristics of non-melanoma skin cancer," Proc SPIE **716102,** 1-9 (2009).

[21] I. Bliznakova, E. Borisova, L. Avramov, "Laser and Light-Induced Autofluorescence Spectroscopy of Human Skin in Dependence on Excitation Wavelengths," Acta Phys Pol A **112,** 1131-1136 (2007).

[22] I. Wang, K. Svanberg, S. Andersson-Engels, R. Berg, S. Svanberg, "Photodynamic therapy of non-melanoma skin malignancies with topical δ-amino levulinic acid: diagnostic measurements," Proc SPIE **2371,** 243-252 (1995).

[23] K. Malzahn, T. Dreyer, H. Glanz, C. Arens, "Autofluorescence endoscopy in the diagnosis of early laryngeal cancer and its precursor lesions," Laryngoscope **112**(3), 488-493 (2002).

[24] M. Zargi, I. Fajdiga, L. Smid, "Autofluorescence imaging in the diagnosis of laryngeal cancer," Eur Arch Otorhinolaryngol **257,** 17-23 (2000).

[25] C. Arens, D. Reussner, H. Neubacher, J. Woenckhaus, H. Glanz, "Spectrometric measurement in laryngeal cancer," Eur Arch Otorhinolaryngol **263**(11), 1001-1007(2006).

[26] O. Aboumarzouk, R. Valentine, R. Buist, S. Ahmad, G. Nabi, S. Eljamel, H. Moseley, S.G. Kata, "Laser-induced autofluorescence spectroscopy: Can it be of importance in detection of bladder lesions?," Photodiagnosis Photodyn Ther **12**, 76-83 (2015).

1. Introduction

Currently, the use of devices emitting light is an indispensable element of many non-invasive diagnostic procedures. Non-invasive fluorescence detection techniques are available for point measurement which provides information useful for monitoring the abundance and location of the fluorophores in low-pigmented superficial neoplasia. These fluorophores could be classified into three main categories: endogenous fluorophores that are responsible for native tissue fluorescence (autofluorescence) like keratin, porphyrins, vitamins and lipids [1,3,5-8]; fluorophores synthetized in the tissue after external administration of a precursor molecule, specifically protoporphyrin IX (PpIX) induced by 5-aminolevulinic acid (ALA) [9]; and fluorophores administrated as exogenous drug such as tetra(m-hydroxyphenyl) chlorin (mTHPC), a typical photosensitizer used in photodynamic therapy (PDT) [10]. In this case, because of the optimal dose during and after PDT are extremely variable [2], the prognosis of PDT treated patients is required. In this vein, it has been reported that fluorescence measurements of PpIX in the skin of patients showed changes in PpIX levels during therapy (photobleaching) and was a good predictor of clinical results [11].

The influence of tissue optics on fluorescence measurements were comprehensively reviewed in literature [12]. Thus, there are important properties that influence fluorescence measurements in tissues, namely, attenuation of light in the tissue, presence of endogenous fluorophores which cause autofluorescence, absorption, scattering, and reflection of light. Light-induced autofluorescence spectroscopy is a very attractive tool for early diagnosis of cancer due to its high sensitivity, easy-to-use methodology for measurements, lack of need for contrast agents' application on the tissue under investigation, possibilities for real time measurements and non-invasive tumor detection [3, 5]. This procedure allows the discrimination between pathological and normal tissue regions based on the differences in the content and metabolic state of a fluorescent compound. Fluorescence measurements are, in principle, straightforward. By filtering the reflected excitation light, it is possible to obtain rather strong signals from the tissues. Problems arise for interpreting the fluorescence signal as the fluorescence peaks are mostly broad and various fluorophores can overlap. Different optical properties in excitation and detection wavelengths also influence the signal. Furthermore, for the excitation wavelength range, generally in the UV region, the penetration depth is a few hundred micrometers, while for detection, the visible region is used, and light can go more than a couple of millimeters. These facts suggest that the intensity of fluorescence cannot be directly interpreted as the corresponding fluorophore concentration. Another consequence is that the measurement configuration, both in excitation and detection, strongly influences not only the signal level but also the shape of the spectrum. Moreover, when the lesion is highly pigmented the obtained fluorescence signal is too weak to be used for diagnostics. In such cases exogenous fluorescent markers could be applied [12,13].

In this work, we develop a violet LED light source suitable for medical application devoted to the diagnostic and treatment of non-melanoma skin cancers. The developed lamp, in combination with a portable spectrometer, is employed to detect differences between the emission spectrum of skin regions with non-melanoma skin cancer and healthy ones at the head of a patient.

2. Materials and methods

2.a. Software for the LED lamp modeling

ZemaxOpticStudio 18.4.1 is a commonly used optical design program used for lighting systems design and image analysis [14-17]. Finished designs of optical devices can be exported as manufacturing-ready results such as ISO drawings and common CAD file formats. We simulated the LEDs source utilizing Blender 2.76 to create a three-dimensional model of the lens and the ZemaxOpticStudio 18.4.1 to describe the light emission performance. For this purpose, the following variables were considered: numbers of simulated rays (n), distance between the source and the sensing surface (z), dimension (12 cm x 12 cm) and number of pixels on the sensing surface (100 x 100 pixels), emission wavelengths of the source, its output power (W), and the light diffusion taken into account through the Lambertian fractions (1/10, 1/12, 0.55/1). Furthermore, we set the wavelength profile for the light source with a central maximum that falls off following a Gaussian curve. Results from simulations were utilized for guiding the LED lamp construction and then the outcome of the real and simulated lamps were compared.

2.b. LED lamp construction and its photometric/radiometric characterization

The LED lamp is constructed employing four 3 W LEDs, coupled to individual lenses and heat sinks. Each LED is fed by an independent electrical circuit with variable electric power to modulate the light intensity.

To characterize the constructed LED lamp, illuminance/irradiance parameters such as irradiance (W/cm^2), radiant power (W) and radiant intensity (W/sr) are determined. For this purpose, an AvaSpec-ULS3648-USB2-UA-25 spectrometer with a CCD detector (3648 pixels) provided with a DUV3648 filter for reduction of second-order effect, and coupled to an optical fiber (200 µm in diameter and 2 m in length) for UV / VIS / NIR range (250- 2500 nm), is utilized. A cosine law CC-VIS / NIR diffuser is adapted to the fiber optic lens. The signal is registered by Avasoft-Full Software. The optical fiber couple to the spectrometer is located at one end of an optical bench, and the light source at a known distance, at the other end of the bench (Fig.1).

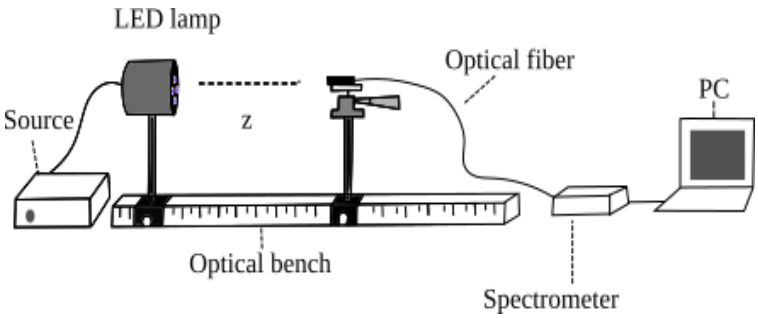

Fig.1. Scheme of the experimental arrangement for characterizing the LED lamp. At one end of the optical bench the LED source is located, and the tip of the fiber optic connected to the spectrometer, is placed at the other end, at a known distance. The spectrometer records the illuminance and allows expressing radiometric analogue units.

2.c. Spectroscopic measurements on the skin of a patient

The lesions on the skin are registered employing a point monitoring system. The excitation light come from the violet LED source developed, and the detection is made by an optical fiber measuring in the 300-800 nm range. The fiber during measurement is supported by hand on the surface of the targeted detection tissue (Fig.2.). For comparison, emission spectra from suspicious skin regions, as well as healthy zones are registered.

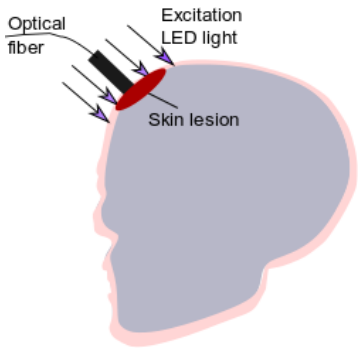

Fig.2. Scheme of the autofluorescence point monitoring system: the excitation is external to the detector, and the detected emission light travels apart through an optical fiber.

3. Results and discussion

3.a. Spectroscopic measurements on the skin of a patient

3.a.a. Modeling

The final light pattern generated by a LED is the result of the sum of the light directly refracted by the encapsulating lens, the light internally reflected inside the lens, and the light from the reflecting cup [18]. The first step to carry out the simulation is to build the emitting source based on a LED and the corresponding lens. Thus, an 8° lens was designed using the Blender 2.76 program. In this software, by drawing the profile of the lens and using the tool "spin", a solid model of revolution was created. The draw lens was exported as CAD file to ZemaxOpticStudio where PMMA for lens material, Lambertian lens type (Lambertian fraction), number of incident rays (n), wavelength, source-surface distance (z) and power, were specified. A scheme of the design process can be seen in Fig.3.

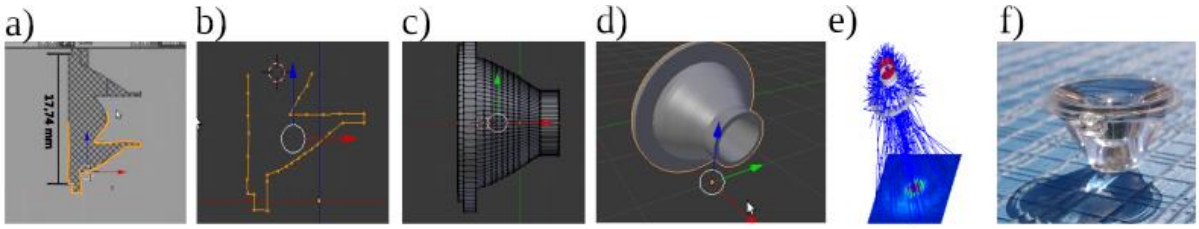

Fig.3. Converging lens design: a) Schematic drawing from lens data sheet; b) drawing the profile using the Blender 2.76 program; c) Application of spin tool to obtain the solid of revolution of the profile drawn in b); d) simulated lens with better definition than c), which was exported to Zemax; e) system of lens-LED in Zemax, and analysis of the emission on a detector surface located at 20 cm of the LED; f) photograph of the real lens.

Multiple variations were tested to model the exit beam of the light source. For example, the radiant intensity is represented for different variables (Fig.4). For n = 50.000 and Lambertian fraction 1/10, the image achieves acceptable definition on the detector surface (Fig.4c).

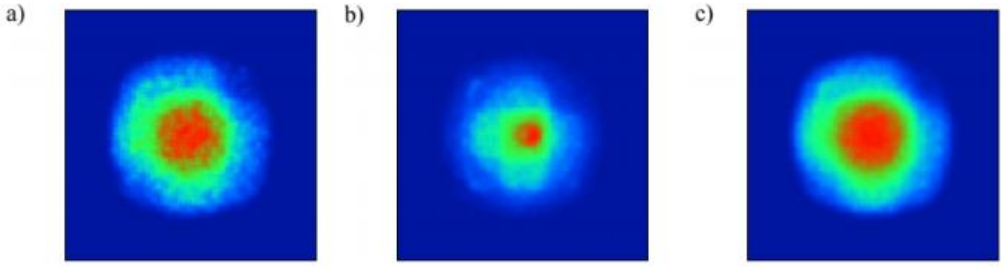

Fig.4. Radiant intensity for different n and Lambertian fractions for z = 20 cm and detector area 12 cm x 12 cm, i.e., 100 x 100 pixels: a) n = 10,000, Lambertian fraction: 1/10; b) n = 50,000, Lambertian fraction: 0.55/1; c) n = 50,000, Lambertian fraction: 1/10.

3.a.b. Construction of the LED lamp

Each 3 W LED coupled to a heat sink and a lens (Fig.5), is mounted on a mobile arm which can be displace in order to focus the lens-LED-heat sink systems on a convenient small region (Fig.6).

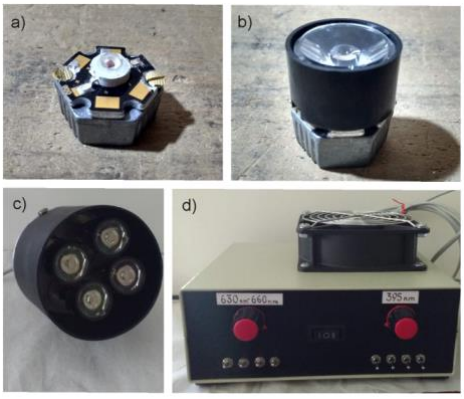

Fig.5. Construction of the LED source with a maximum total power of 12W achieved with four 405 nm violet LEDs of 3 W each. a) LED-heat sink system. A 3 W high power LED is coupled to a single heat sink; b) lens-LED-heat sink system, made up of a lens of 8º coupled to the LED-heat sink system; c) photograph of the 12W LED lamp with all four lens-LED-heat sink systems. d) 12W LED lamp power supply, with the possibility of turning on one, two, three or four LEDs simultaneously. Furthermore, it is possible to regulate the intensity of each LED and thus the overall source output.

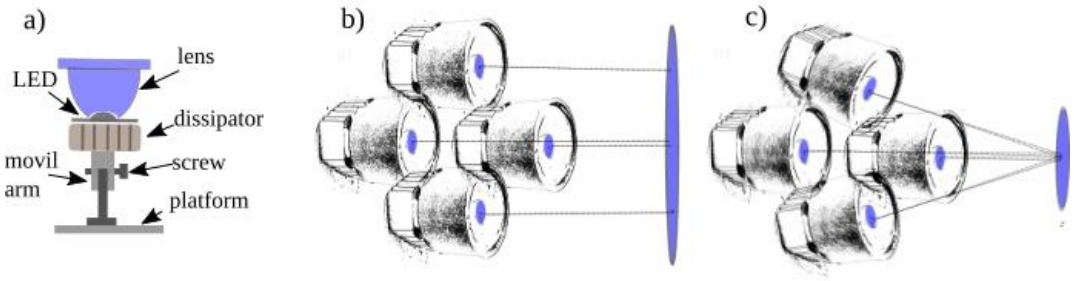

Fig.6. a) Scheme of a single LED system consisting of a LED with an 8 degree lens coupled to the LED-heat sink on a mobile arm; b) Four LEDs in the parallel configuration; c) Four focused LEDs.

3.a.c. Comparison between simulated and constructed LED lamp

The real image of the illumination area generated by the LED source with central axis-oriented lenses at 20 cm distance is shown in Fig.7a and Fig.7b. And the illuminated areas generated by the simulated sources with and without lenses are depicted in Fig.7c and Fig.7d, respectively. The schematic arrangements of the LEDs for the simulations are also include in the figure (Figs.7e and f).

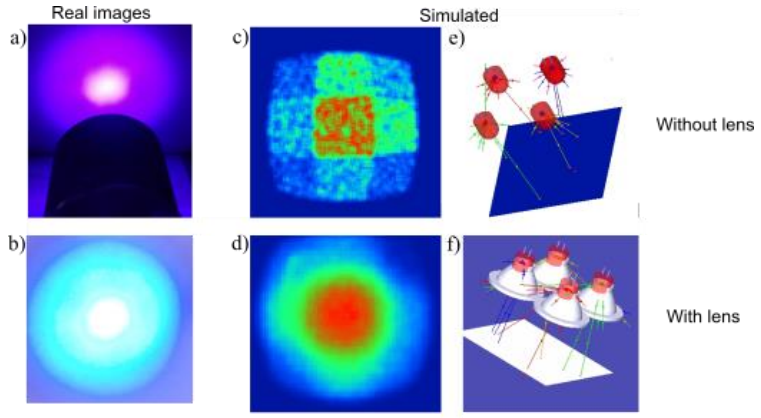

Fig.7. a) Comparison of real lamp with simulated lens-LEDs. a) photography of violet LED lamp with central axis-oriented lenses; b) photograph of the area illuminated by the LED lamp with focused lenses at 20 cm from the source; c) radiant intensity on the 100 x 100 pixels (24 cm X 24 cm) detector surface without lenses; d) radiant intensity on the 100 x 100 pixels (24 cm X 24 cm) detector surface with lenses; e) four LEDs without lenses located at z = 20 cm; f) four LEDs with 8° lenses located at z = 20 cm.

In another set of experiments, we obtained the simulated irradiance from the source (W/cm^2) for different Lambertian fraction and compared it with the irradiance measurement with the spectrometer described in figure 1 for the constructed LED lamp. For a Lambertian fraction 1/10, simulated results did not fit experimental observations, but changing it to 1/12, experimental data could be reproduced (Fig. 8a). An appropriate agreement was obtained between the simulation and the experiment in verifying the inverse-squared law, by measuring the irradiance for different distances (d) between the detector and the LED lamp with the experimental arrangement depicted in the scheme showed in figure 1 (Fig. 8b).

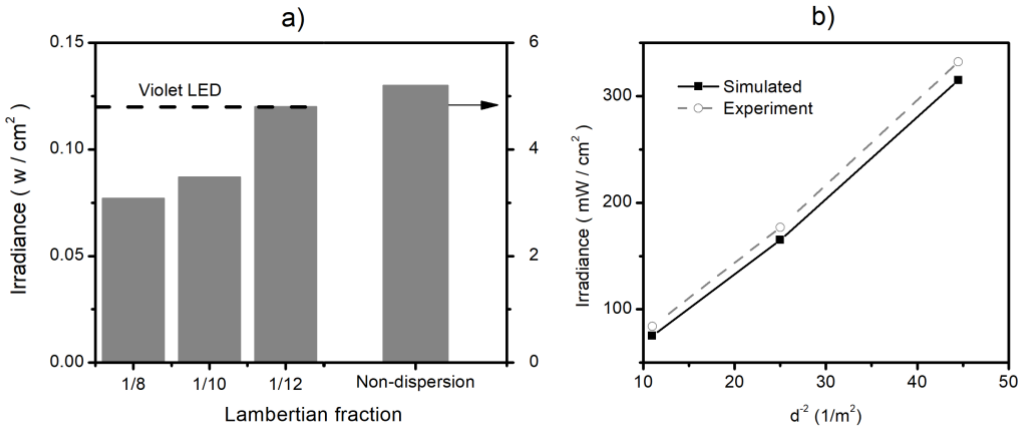

Fig. 8. a) Irradiance for different Lambertian fractions. Comparison between the simulated violet LED lamp (vertical bars) with the physical measurement (horizontal dashed line); b) Comparison between simulated and measured irradiance as a function of $1 / d^2$ for the LED lamp.

3.b. *Application of the violet LED source to detect non-melanoma skin cancer*

As know, the PpIX exhibits maximum light absorption (the Soret peak) at 405 nm and an emission peak in the red region. PpIX concentration is expected to be increased in pathological skin [19]. For this propose,

we used the constructed violet LED lamp with maximum excitation peak at 405 nm to illuminate suspicious points in the head of a patient with a non-melanoma skin cancer before (Fig. 9a) and after (Fig. 9b) the treatment with a red medical laser emitting at 652 nm.

The fluorescence intensity of the PpIX was recorded with a spectrometer couple to an optical fiber with the scheme showed in figure 2. The average spectrum from suspicious areas as well as regions of healthy skin exhibits an emission peak at 505 nm, being the intensity of suspicious points greater than healthy skin area. Furthermore, suspicious points exhibit another structured peak in the 600 - 700 nm range (Fig. 9c, black squares). The later feature appears as a shoulder for the case of the average emission spectrum taken from the hand skin (Fig. 9c, red squares) or from different treated points at the head (Fig. 9d). A reference curve can be obtained from the decaying tail of the peak at 505 nm to be subtracted from emission intensity at the 550 – 700 nm range [20]. The inset in Fig. 9c shows a rather clear peak, while a noisy signal is obtained for red laser treated regions (inset in Fig. 9d). This description is consistent with the increased amount of PpIX in pathological regions in comparison with a healthy skin and treated regions. A similar interpretation has been proposed in literature [21].

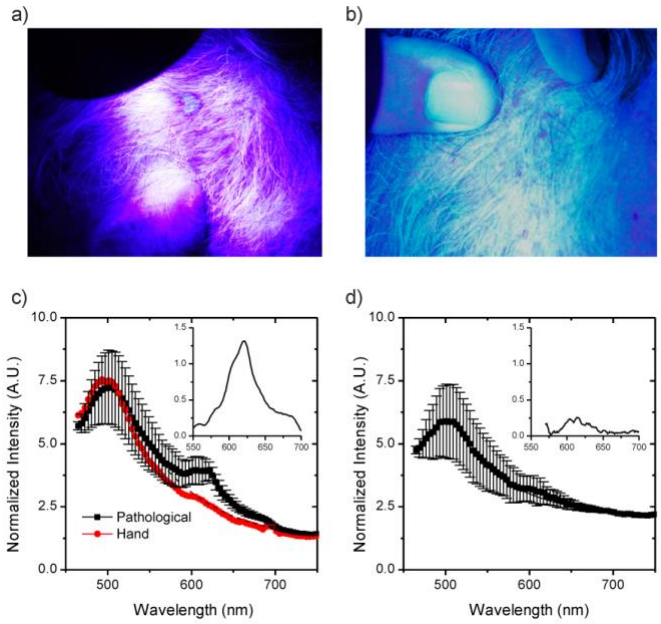

Fig.9. PpIX fluorescence decrease after treatment with red laser. (a and b) Photographs of the lesion at the head of a patient before (a) and after (b) the treatment with a clinical red laser source. (c) Average fluorescence spectrum from lesions before treatment (black circles), and fluorescence spectrum from the skin of the hand (red circles) taken as healthy skin. The reference curve obtained from the decaying tail of the peak at 505 nm is shown in dashed lines. (d) Fluorescence spectrum from treated lesions. Insets show a significant decrease in the intensity peak in the 600 – 700 nm range related to PpIX. The peaks can be more clearly appreciated after subtracting the reference curve.

Fluorescence spectroscopy with 405 nm excitation for the detection of non-melanoma tumors in vivo, has been reported in literature [4]. In this work, authors have demonstrated the correlation between cancer detection diagnostic accuracy and skin phototype of the patient. With increasing of cutaneous pigmentation, the diagnostic accuracy for tumor detection and differentiation from normal skin fall down. In our case, we followed the fluorescence on a patient with non-melanoma neoplastic disease before and after the treatment. It can be detected a significant decrease in the fluorescence in the 600 – 700 nm range, for treated regions (Figure 9). We employed a point monitoring system like that employed in reference [22]. There, the pharmacokinetics of PpIX in skin tumors, i.e., basal cell carcinomas (BCC) and T-cell lymphomas, and normal skin utilizing a laser induces fluorescence for the in vivo point monitoring of the lesion surface and the surrounding normal skin, has been studied. In this research, laser light at 652 nm was used and the fluorescence emission spectra detected showed information about the build-up of the PpiX and the tumor selectivity in the superficial layers of the area planned for treatment.

4. Conclusions

At present, histochemical methods are the standard procedures in diagnosis of many disorders, primarily neoplastic ones. However, autofluorescence-based techniques applied to tissue analysis can be performed

in real time because it does not require any treatment of fixing or staining of the tissue. Most authors, who used autofluorescence in diagnostics of precancers and malignant tumors, have declared as drawbacks, that there was relatively high rate of false-positive findings [23-25]. Is possible to find unexpected false positive may be caused by the appearance of a minimal amount of blood (hemoglobin) on surface, bacterial colonization [26], inflammation, edema, as well as scar formations. In any case, autofluorescence based strategies, due to their easy implementation in the clinic, are convenient for screening purpose.

In this work we describe the modeling, the construction and characterization of a violet LED light source with controlled power, and which can be focused on a small surface region, achieving and irradiance of 165 mW cm^{-2} at 25 cm from the source. Furthermore, the application of the LED source to the follow up of a non-melanoma skin cancer was reported. The fluorescence spectra from tumors and normal surrounding tissue regions illuminated by the developed UV/violet LED lamp, was registered employing a portable spectrometer and an optical fiber probe. Fluorescence spectra were recorded pre- and pos-treatment with a clinical laser source. PpIX enhanced concentration was detected in pathological skin areas according to corrected fluorescence spectra.

The present work suggests that changes in the fluorescence spectrum characteristics could be mainly relate to appearance or concentration changes in fluorophores, which are presented in a given skin pathology, and could be associated to changes in metabolic activity of given tissue. These results would be valuable in the design of photodynamic diagnostic protocols as well as for together with the improving the control of treatment dosing, both as a single or adjuvant intervention, making these alternative approaches more attractive for clinical massive application.

Acknowledgement

This work was supported by the Consejo Nacional de Investigaciones Científicas y Técnicas (CONICET, Argentina) and Universidad Nacional de La Plata (Grant No. 11/X900). M.A.P. is staff member of CONICET.